Characterization of Urinary Calculi Using Laser-Induced Breakdown Spectroscopy and X-ray Diffraction: A Regional Study in Iran

Rezvan Babamir , Mohammad Ali Haddad^{a,b,*}, Seyed Hassan Tavassoli^c, Mohamad Reza Samadzadeh Yazdi^d, and Serajoddin Vahidi^e

aDepartment of Physics, Yazd Univeristy, Yazd, Iran
bLaser Spectroscopy Research Laboratory, Yazd Univeristy, Yazd, Iran
cLaser and Plasma Research Institute, Shahid Beheshti University, Tehran, Iran
dDepartment of Mining and Metallurgical Engineering, Yazd University, Yazd, Iran
Andrology Research Center, Yazd Reproductive Sciences Institute, Shahid Sadoughi
University of Medical Sciences, Yazd, Iran

*Corresponding author email: mahaddad@yazd.ac.ir

Received: Apr. 17, 2025, Revised: June 6, 2025, Accepted: June 11, 2025, Available Online: June 13, 2025, DOI: will be added soon

ABSTRACT—Detailed compositional analysis of kidney stones is crucial for effective treatment and prevention; however, region-specific data are often limited. This study aimed to characterize the composition of urinary stones in Yazd Province, Iran, where such information is required. Urinary stones from 40 patients in Yazd were analyzed using Laser-Induced Breakdown Spectroscopy (LIBS) for elemental identification and X-ray Diffraction (XRD) for crystalline structure determination. LIBS was applied to both macroscopically uniform and heterogeneous stones to assess the intra-stone variability in elemental composition. LIBS revealed the consistent prominence of carbon, calcium, and nitrogen in uniform stones. exhibited heterogeneous Notably, stones significant intra-stone variations in elemental composition. XRD identified key crystalline components, including calcium oxalate (whewellite and raphide), calcium carbonate (calcite), and uric acid (uracite). These findings offer region-specific understanding into the types and characteristics of urinary stones prevalent in Yazd, Iran, emphasizing the **importance** of considering intra-stone heterogeneity. The integration of LIBS and XRD offers a comprehensive approach to stone characterization. Further research correlating findings with patient-specific environmental factors in Yazd is warranted to

improve our understanding and treatment strategies.

KEYWORDS: Elemental analysis, Heterogeneity, Kidney stones, Laser-Induced Breakdown Spectroscopy (LIBS), X-ray Diffraction (XRD).

I. Introduction

Kidney stones are a major global health concern owing to their painful manifestations and potential for severe complications including urinary tract obstruction and renal damage. Elemental analysis of kidney stones is essential to understand their formation and composition, which can inform appropriate treatment strategies. Spectroscopic techniques, such as Laser-Induced Breakdown Spectroscopy (LIBS), Raman spectroscopy, Fouriertransform infrared spectroscopy (FTIR), and spectrum-domain computed tomography (SDCT), have markedly improved kidney stone analyses, offering detailed insights into their compositions and structures, which can assist in diagnosis, treatment, and prevention. [1-4]. These techniques have significant medical applications because of their ability to provide detailed and rapid analysis of biological tissues. This technology exploits the interaction between laser light and biological samples to

detect and analyze their properties, rendering it various diagnostic invaluable for therapeutic applications. FTIR and X-ray Diffraction (XRD) have been extensively employed ascertain the chemical composition and crystalline structure of kidney stones [5]. FTIR facilitates chemical mapping, revealing the distribution of compounds within the stones, whereas XRD provides insight into their crystalline structures. These methods are essential for understanding the etiology of nephrolithiasis and developing effective preventive strategies [6]. Raman chemical imaging is an innovative methodology that generates two-dimensional representations of the constituent distribution within kidney stones. This method aids in detecting different chemical constituents, like calcium oxalate and uric acid, and provides understanding of their spatial arrangement within stones.[7]. Raman chemical imaging, although time intensive, provides high accuracy and is particularly advantageous for research purposes. Spectral Detector Computed Tomography (SDCT) is a non-invasive imaging modality that facilitates the differentiation of kidney stones based on their characteristics [8]. This method facilitates semi-automatic segmentation and sophisticated image post-processing of stones, even at reduced radiation levels, making it a valuable tool in clinical settings. SDCT can differentiate between calcific and non-calcific stones, thereby aiding in precise diagnosis treatment planning [9].

In addition to the methods mentioned above, another study employed neutron activation investigate analysis the elemental to compositions of calcium oxalate, uric acid, and xanthine in kidney stones. This analysis identified elements, such as Al (Aluminum), Au (Gold), Br (Bromine), Ca (Calcium), Cl (Chlorine), Co (Cobalt), Cr (Chromium), Fe (Iron), Hg (Mercury), I (Iodine), K (Potassium), Mg (Magnesium), Na (Sodium), (Antimony), Se (Selenium), Sr (Strontium), and Zn (Zinc). Calcium oxalate stones exhibit higher concentrations of these elements than uric acid and xanthine stones do [10]. Protoninduced X-ray emission (PIXE) analysis of recurrent calcium oxalate kidney revealed trace elemental patterns, with positive levels correlations among the of (Manganese), Fe (Iron), Cu (Copper), Zn (Zinc), Sr (Strontium), and Ca (Calcium). Furthermore, inductively coupled plasma optical emission spectrometry (ICP-OES) has identified the presence of elements such as Ba (Barium), Ca (Calcium), Cu (Copper), Fe (Iron), K (Potassium), Li (Lithium), Mg (Magnesium), Mn (Manganese), Na (Sodium), P (Phosphorus), Sr (Strontium), and Zn (Zinc) in kidney stones. The observed correlations between these elements suggest their potential role in the formation of kidney stones [11]. This method facilitates the understanding of the mechanisms underlying kidney stone induction and growth. [12]. Among the aforementioned methodologies, LIBS has been used in various applications [13], [14], including biomedical applications such as the analysis of both hard and soft tissues, identification and classification of pathogenic agents, and laser-guided surgical procedures. LIBS and Raman Spectroscopy are analytical methods that work well together to offer both elemental and molecular insights into the makeup of kidney stones. LIBS is proficient in detecting elements such as carbon, calcium, hydrogen, and oxygen, whereas Raman Spectroscopy facilitates the differentiation of various kidney stone types based on their molecular structures. These methodologies are particularly advantageous for identifying the primary constituents of kidney stones, which frequently comprise a single predominant compound [15]. LIBS has been employed to analyze hard tissues such as teeth and bones, offering detailed elemental mapping that is crucial for understanding conditions such as osteoporosis and dental caries. [7]. This technique has demonstrated efficacy in the analysis of soft tissues and various biomedical specimens, providing a reagent-free real-time approach for the detection and characterization of biological materials. [2], [7], [16]. The integration of LIBS with machine learning has demonstrated potential in minimally invasive diagnostic applications, particularly differentiating healthy tissues from diseased tissues through elemental fingerprinting. [17].

LIBS has numerous advantages in the analysis of kidney stones, rendering it a valuable tool in medical diagnostics and research. LIBS is particularly effective for kidney stone analysis because of its capacity to rapidly and accurately ascertain elemental composition [18]-[20], with minimal sample preparation [19]. Its nondestructive nature and cost-effectiveness [15], coupled with its ability to detect toxic elements [20], make it a favorable option for clinical diagnostics and research on the prevention and treatment of nephrolithiasis. This technique facilitates analysis of the spatial distribution of elements within stones, thereby providing insights into the growth and formation processes of kidney stones [1], [21]. LIBS was used to conduct an in situ quantitative analysis of the elemental composition of various kidney stone sections. The elements that were identified include Calcium (Ca), Magnesium (Mg), Manganese (Mn), Copper (Cu), Iron (Fe), Zinc (Zn), Strontium (Sr), Sodium (Na), Potassium (K), Carbon (C), Hydrogen (H), Nitrogen (N), Oxygen (O), Phosphorus (P), Sulfur (S), and Chlorine (Cl). The investigation revealed differences in elemental concentrations across distinct regions of stones and among stones from different age groups [21]. These techniques were utilized to analyze 83 kidney stone samples, allowing for the identification of P (Phosphorus), K (Potassium), Ca (Calcium), Fe (Iron), Zn (Zinc), Ni (Nickel), Br (Bromine), (Strontium), and Pb (Lead). Various crystalline substances such as apatite, struvite, uric acid, weddellite, whewellite, magnesium phosphate, and calcium phosphate were detected. This thorough examination enhanced the understanding of the composition and development of kidney stones.[5]. LIBS, in conjunction with XRD and X-ray fluorescence (XRF), has been employed for the classification and analysis of kidney stones [19]. LIBS has been used to identify the carcinogenic metals present in kidney stones. The detection of elements such as Cr (Chromium), (Cadmium), Pb (Lead), Zn (Zinc), phosphate, and V (vanadium) contributes to a deeper understanding of the potential health risks associated with kidney stones. [20]. A comparative study demonstrated that LIBS is a

proficient method for analyzing urinary stones, yielding results comparable to those obtained through X-ray diffraction. LIBS is noted for its straightforwardness, affordability, and nondestructive nature, making it ideal for regular use [15]. A thorough review of the applications of LIBS in biomaterial analysis, including kidney stones, highlights its versatility and robustness as an analytical tool. This review examines the use of LIBS for multi-elemental analysis and highlights its advantages over traditional techniques [22]. An article reviewed the use of LIBS in analyzing urinary stones, focusing on its quick and non-invasive nature. This review underscores LIBS's ability to offer comprehensive spatial distribution elements within stones, thus aiding in a better comprehension of stone formation and plant growth [1].

Investigation of the prevalence of kidney stones in Iran has identified multifaceted interactions between metabolic, dietary, and socioeconomic factors contributing to their occurrence. Implementing targeted public health strategies and personalized medical interventions may substantially alleviate the burden of kidney stone diseases in this region. Kidney stones are prevalent in Iran, with research indicating significant incidence rates in different regions. Prominent risk factors include hypertension, obesity, diabetes, and lifestyle practices such as alcohol and opium consumption [23],[24]. Both socioeconomic and environmental determinants contribute to the incidence of kidney stones [25]. In contrast to Western countries, where hypercalciuria is prevalent, Iranian patients frequently present with low urine Vol.ume and hypocitraturia as primary metabolic abnormalities [24]. These findings underscore the need for dietary and lifestyle interventions tailored to specific regions worldwide. In Iran, the mineral composition of kidney stones frequently includes calcium oxalate, uric acid, and phosphate. The notable presence of trace elements such as zinc and strontium suggests potential environmental influences on stone formation [26], [27]. A diet characterized by pro-inflammatory properties is associated with chronic kidney disease, although it does not directly correlate with kidney stone formation. This underscores the significance of dietary management preventing kidney-related disorders Socioeconomic disparities in the prevalence of kidney stones indicate that public health interventions should account for these inequalities to enhance their effectiveness [25].

Studying kidney stones among Yazd, Iran residents, is crucial because of the high occurrence of kidney stone disease in this region. Understanding the composition and characteristics of these stones can provide valuable insights into their risk factors and preventive strategies. The mineral composition and trace element content of kidney stones can differ depending on geographical location, diet, and other environmental factors. Analyzing stones from the Yazd inhabitants may reveal unique patterns that are specific to this region. Such analyses can reveal the underlying metabolic abnormalities common in the Yazd population, which differ from those observed in Western countries. Detailed compositional analysis aids in determining the appropriate treatment approaches and preventive measures. Identifying trace elements in stones may highlight potential environmental the influences on stone formation.

This study aimed to investigate the composition and heterogeneity of urinary stones collected from patients in Yazd Province, Iran, using LIBS for rapid and minimally destructive elemental analysis, and X-ray Diffraction (XRD) for crystalline structure determination. A key goal is to establish detailed elemental profiles, including trace elements, directly from these stones and lay the groundwork for understanding stone formation processes specific to the Yazd region. Furthermore, this study proposes a systematic elemental analysis of water, soil, and food sources in Yazd with the aim of correlating environmental exposure with the observed trace element composition of kidney stones. By uniquely combining **LIBS** technology, comprehensive environmental assessment, and consideration of socioeconomic factors, this study sought to provide a holistic understanding of kidney stone formation specific to Yazd, Iran, ultimately contributing to tailored intervention strategies for this high-risk population. These findings are expected to offer valuable insights into the characteristics of kidney stones in Yazd, including intra-stone elemental variability, with significant implications for developing region-specific clinical management and prevention strategies for kidney stones.

II. EXPERIMENTAL PROCEDURE

A. Sample Preparation

Forty kidney stone samples were obtained from patients following surgical removal at Yazd Shahid Rahnemuon Hospital in collaboration with the hospital's surgical department. The collected kidney stone samples underwent a multistage preparation process that meticulously tailored to the requirements of the specific spectroscopic techniques employed. Upon collection, the stones were rinsed with saline solution and thoroughly washed with deionized water. This procedure was performed remove any residual biological contaminants, including urine and blood clots, that might have been present in the samples. The cleaned samples were dried at ambient temperature and stored individually hermetically sealed containers to prevent contamination or degradation. Figure 1 shows the images of 40 kidney stone samples that exhibited variations in shape, color, and texture.

For Fourier transform infrared spectroscopy (FTIR) and X-ray Fluorescence analyses, the entirety of each stone or representative fragment was comminuted into a fine powder using a mortar and pestle. The resultant powder was used directly for FTIR analysis in transmittance mode. For XRF analysis, the powder was processed according to the requirements of the XRF spectrometer. LIBS requires a considerably less complex sample preparation protocol: cleaned and desiccated stones are sectioned in half using a clean and sharp blade.

This procedure was performed to expose the internal structure of the stone, thereby facilitating spatially resolved analysis with

specific targeting of the stone core, intermediate layers, and the outer surface.

Unlike AAS and ICP-MS, LIBS does not require further processing.

Sample1 Sample2 Sample3 Sample4 Sample5 Sample6 Sample7 Sample8 Sample9 Sample10 Sample11 Sample12 Sample13 Sample14 Sample15 Sample15 Sample16 Sample17 Sample18 Sample19 Sample20 Sample20 Sample21 Sample22 Sample23 Sample24 Sample25 Sample26 Sample26 Sample27 Sample28 Sample29 Sample30 Sample36 Sample37 Sample38 Sample39 Sample39 Sample40					
Sample6 Sample7 Sample8 Sample9 Sample10 Sample11 Sample12 Sample13 Sample14 Sample15 Sample16 Sample17 Sample18 Sample19 Sample20 Sample21 Sample22 Sample23 Sample24 Sample25 Sample26 Sample27 Sample28 Sample29 Sample30 Sample31 Sample32 Sample38 Sample39 Sample35		Surla	Samula 2		Sample
Sample11 Sample12 Sample13 Sample14 Sample15 Sample16 Sample17 Sample18 Sample19 Sample20 Sample21 Sample22 Sample23 Sample24 Sample25 Sample26 Sample27 Sample28 Sample29 Sample30 Sample31 Sample32 Sample33 Sample34 Sample35 Sample36 Sample37 Sample38 Sample39 Sample40	Sample1	Sample2	Sample3	Sample4	Samples
Sample11 Sample12 Sample13 Sample14 Sample15 Sample16 Sample17 Sample18 Sample19 Sample20 Sample21 Sample22 Sample23 Sample24 Sample25 Sample26 Sample27 Sample28 Sample29 Sample30 Sample31 Sample32 Sample33 Sample34 Sample35 Sample36 Sample37 Sample38 Sample39 Sample40	•				9
Sample11 Sample12 Sample13 Sample14 Sample15 Sample16 Sample17 Sample18 Sample19 Sample20 Sample21 Sample22 Sample23 Sample24 Sample25 Sample26 Sample27 Sample28 Sample29 Sample30 Sample31 Sample32 Sample33 Sample34 Sample35 Sample36 Sample37 Sample38 Sample39 Sample40	Sample6	Sample7	Sample8	Sample9	Sample10
Sample21 Sample22 Sample23 Sample24 Sample25 Sample26 Sample27 Sample28 Sample29 Sample30 Sample31 Sample32 Sample33 Sample34 Sample35 Sample36 Sample37 Sample38 Sample39 Sample40			*		
Sample21 Sample22 Sample23 Sample24 Sample25 Sample26 Sample27 Sample28 Sample29 Sample30 Sample31 Sample32 Sample33 Sample34 Sample35 Sample36 Sample37 Sample38 Sample39 Sample40	Sample16	Sample17	Sample18	Sample19	Sample20
Sample26 Sample27 Sample28 Sample29 Sample30 Sample31 Sample32 Sample33 Sample34 Sample35 Sample36 Sample36 Sample37 Sample38 Sample39 Sample39	- Sumprove				
Sample26 Sample27 Sample28 Sample29 Sample30 Sample31 Sample32 Sample33 Sample34 Sample35 Sample36 Sample36 Sample37 Sample38 Sample39 Sample39			6		
Sample31 Sample32 Sample33 Sample34 Sample35 Sample36 Sample37 Sample38 Sample39 Sample40	Sample21	Sample22	Sample23	Sample24	Sample25
Sample31 Sample32 Sample33 Sample34 Sample35 Sample36 Sample37 Sample38 Sample39 Sample40	S. Loc	Samula 27	Samula 22	Sample 20	Samula 20
Sample36 Sample37 Sample38 Sample39 Sample40	Sample26	Sample2/	Sample28	Sample29	Sample30
Sample36 Sample37 Sample38 Sample39 Sample40	•			00	
Sample36 Sample37 Sample38 Sample39 Sample40	Sample31	Sample32	Sample33	Sample34	Sample35
	•	0			T
					Sample40

Fig. 1. Images of 40 kidney stone samples showing variations in shape, color, and texture.

B. LIBS Experimental Setup

The LIBS experiments for the analysis of gallstones and kidney stones employed a configuration similar to that described previously. Figure 2 shows the optical array of LIBS used in our measurements. The principal components of the LIBS system comprised a Nd:YAG laser as the plasma generation source, plasma collection optics, spectrometer, and data acquisition system. The laser was operated at

1064 nm and delivered a maximum pulse energy of \sim 70 mJ (pulse duration of \sim 10 ns pulse duration) at a 1 Hz repetition rate of 1 Hz. The laser beam, with a diameter of \sim 2 mm was focused on the sample surface using a quartz lens with a focal length of 15 cm, resulting in a laser fluence of \sim 2 \times 10² J cm⁻² on the surface of each stone sample. The light emitted from the laser-induced plasma was collected using an optical fiber bundle, often

with a lens to enhance the collection efficiency, and directed to an Echelle spectrometer equipped with an ICCD camera for spectral dispersion and detection over the wavelength range of 200 nm to 1000 nm.

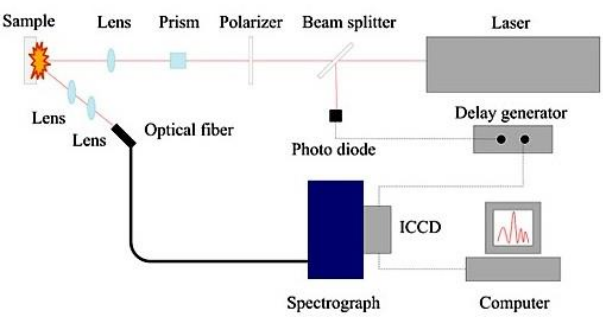


Fig. 2. Scheme for LIBs setup

The LIBS spectra are often recorded with a specific gate delay (e.g., 1.5 µs for analysis). To improve the signal-to-noise ratio, the spectra were averaged over multiple laser shots (e.g., 10 shots for the stone analysis). In spatial distribution studies, single-shot LIBS spectra are sometimes acquired to mitigate sample degradation. The samples were positioned on a translatable platform (x–z stage or rotary table) to enable the laser beam to focus on different points of interest and ensure that each laser pulse irradiated a fresh portion of the sample.

III.RESULTS AND DISCUSSION

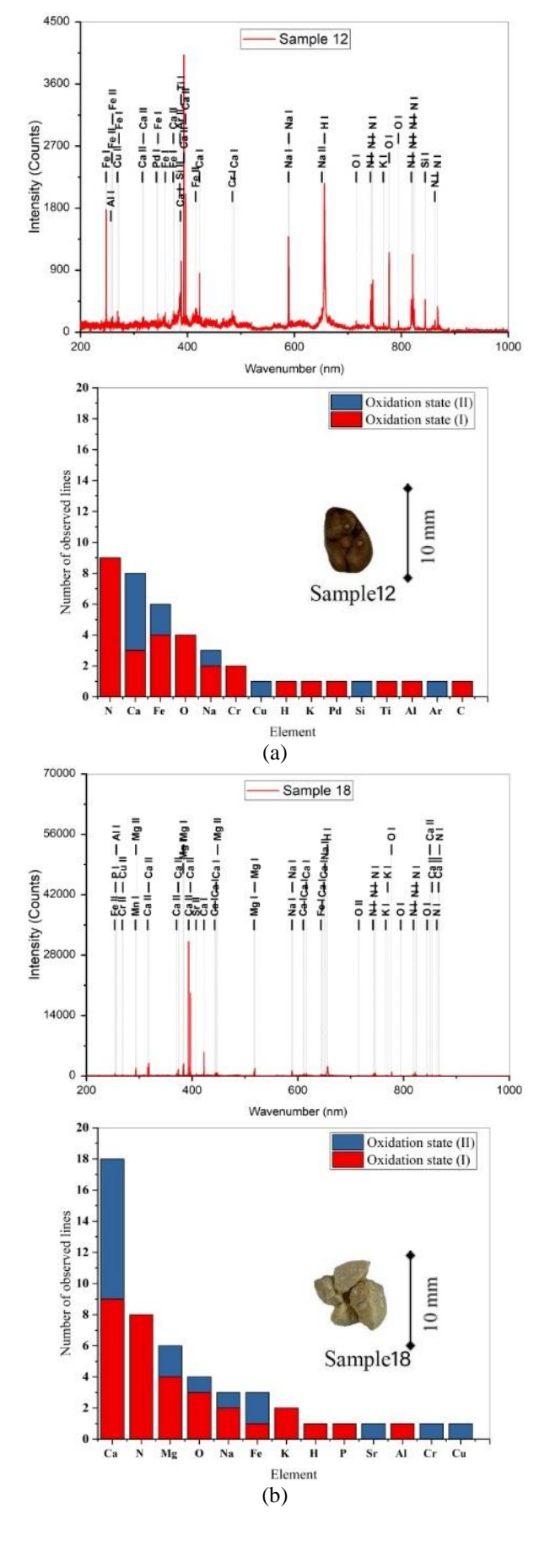
The results obtained from The LIBS analysis was performed on a collection of urinary tract stone samples. The primary objective of employing LIBS was to conduct comprehensive elemental characterization of these stones, providing valuable insights into their fundamental composition. This study included 40 urinary stone samples obtained from patients with urolithiasis. Given the observed diversity in the macroscopic characteristics of the collected samples, LIBS analysis was performed in two distinct phases. This phased approach was designed to systematically investigate both seemingly homogeneous and visibly heterogeneous stone specimens, allowing for a more precise understanding of their elemental composition.

A. Elemental Composition of Macroscopically Uniform Urinary Stones

The initial phase of LIBS analysis focused on a subset of 28 urinary stone samples that exhibited macroscopic uniformity in their physical attributes, including shape, texture, and coloration. The rationale for selecting these seemingly homogeneous samples was to establish a foundational understanding of the elemental constituents prevalent in urinary calculi that did not present obvious visual differences. For each of the 28 samples, the LIBS spectra were acquired from a single representative location on the stone surface. This sampling strategy was based on the assumption that visually consistent stones would exhibit a relatively uniform elemental distribution throughout the bulk material. To ensure the removal of superficial contaminants such as urine, blood residues, or dust particles present on the stone surfaces, the first two laser pulses directed at each sampling point were discarded from the analysis. The final LIBS spectrum for each analysis location was obtained by averaging the spectra of the five consecutive laser pulses Analysis of acquired **LIBS** spectra for 28 the macroscopically uniform stone samples revealed the consistent presence of a specific suite of elements across a significant proportion of the analyzed groups. The elements detected through their unique emission lines included carbon (C), calcium (Ca), chromium (Cr), copper (Cu), iron (Fe), hydrogen potassium (K), magnesium (Mg), nitrogen (N), sodium (Na), oxygen (O), phosphorus (P), palladium (Pd), silicon (Si), tin (Sn), strontium (Sr), thorium (Th), titanium (Ti), aluminum (Al), argon (Ar), barium (Ba), zinc (Zn), and zirconium (Zr).

Figure 3 presents the LIBS spectra and the corresponding elemental composition analysis of the three-kidney stone samples (a) 12, (b) 18, and (c) 20. The top panels display the LIBS spectra, showing the characteristic emission peaks of the detected elements and their respective assignments. The bottom panels illustrate the distribution of the identified elements in different oxidation states (blue:

ionization state II, red: ionization state I) along with sample images for visual reference.



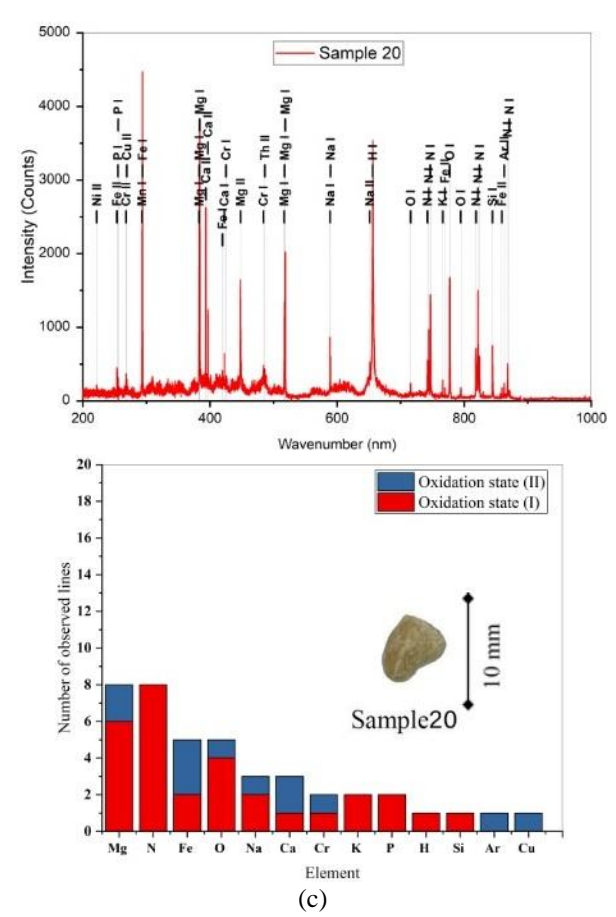


Fig. 3. LIBS spectra (top) and elemental composition analysis (bottom) of kidney stone samples (a) 12, (b) 18, and (c) 20, highlighting key elements and oxidation states

The elemental composition highlights key constituents such as calcium (Ca), nitrogen (N), magnesium (Mg), and iron (Fe), which are commonly associated with kidney stone formation. These elements were identified by comparing meticulously the observed wavelengths of the emission lines in the LIBS spectra with the extensive spectral databases maintained by organizations AtomAnalyzer (AtomTrace, Czech Republic) and NIST [29]. To ensure accurate elemental assignments, a small tolerance window was considered to account for minor variations in the wavelength owing to plasma conditions or instrumental factors. Furthermore, the reported upper and lower energy levels associated with the identified atomic and ionic transitions were cross-referenced with the database information to provide additional confidence in elemental identification. Among the identified elements, certain species exhibited particularly prominent and frequently observed emission lines in the

LIBS spectra of the 28 samples. For instance, strong and readily identifiable emission lines corresponding to sodium (Na) were consistently detected at 588.99 nm and 589.59 nm. Similarly, the characteristic emission lines of calcium (Ca) were frequently observed at 393.37, 396.85, 422.67, 315.88, and 317.93 nm. Additionally, emission lines indicative of the presence of nitrogen (N) were found at 742.36, 744.23, 746.83, and 656.28 nm.

The regular identification of these elements is particularly significant, as Sodium (Na), Calcium (Ca), and nitrogen, along with oxygen

and carbon (which are frequently inferred or indirectly identified in LIBS of complex matrices), are recognized as primary components of various types of urinary stones, such as calcium oxalate, calcium phosphate, and uric acid stones. A summary of the XRD and LIBS results of the selected samples is presented in Table 1. Elemental analysis detected major and trace elements including Ca (Calcium), N (Nitrogen), Fe (Iron), O (Oxygen), Na (Sodium), Si (Silicon), Ti (Titanium), and Cu (Copper), providing a detailed chemical composition of the samples.

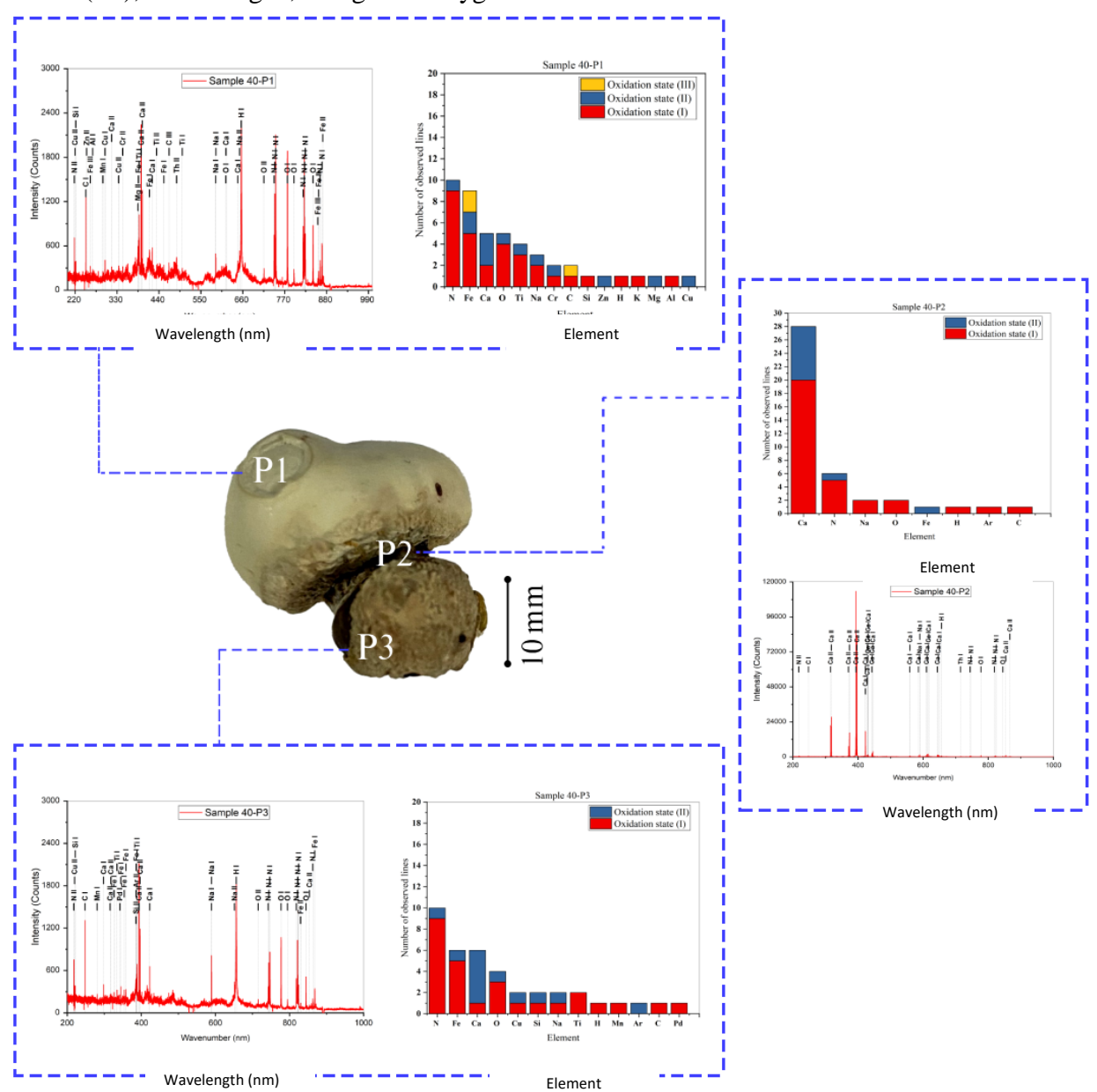


Fig. 4 Image of a kidney stone (Sample 40) with three distinct regions (P1, P2, and P3), accompanied by their corresponding elemental analysis and spectral data.

B. Intra-Stone Elemental Variability in Macroscopically Heterogeneous Urinary Stones

The second phase of the LIBS analysis was dedicated to the investigation of 12 urinary displayed samples that visible macroscopic heterogeneity in terms of color, material composition (e.g., presence of distinct layers or regions with different textures), and overall shape (similar to sample 40 in Fig. 1). These samples were selected to explore the possibility variations elemental of in composition within a single urinary stone. For each of the 12 heterogeneous samples, LIBS spectra were acquired from multiple distinct locations on the stone surface, typically at two or three points. This multipoint analysis strategy was designed to create a rudimentary elemental map of each heterogeneous stone, identification allowing for the characterization of any localized compositional differences that might exist within the same sample. The experimental parameters of the LIBS analysis conducted heterogeneous samples are consistent with those employed in the first phase of this study. The LIBS spectra acquired from each sampling point were subjected to the same rigorous processing spectral and elemental identification, inVol.ving a comparative analysis with standard spectroscopic databases and relevant literature. Figure 4 shows an image of a composite kidney stone (Sample 40) with three distinct regions (P1, P2, and P3) along with their corresponding elemental analysis and spectral data. LIBS analysis of these 12 macroscopically heterogeneous samples yielded a significant and crucial finding: considerable variations in elemental composition were observed across different sampling points within individual stones. Although many of the elements identified in the macroscopically uniform samples were also detected in these heterogeneous specimens, the relative intensities and even the presence or absence of specific emission lines exhibited substantial differences depending on the exact location of the analyzed stone. Notably, in addition to the previously identified elements, such manganese elements as

molybdenum (Mo), nickel (Ni), and bromine (Br) were also detected in some of the heterogeneous samples, and their presence was often localized to specific regions within the stone. For instance, several heterogeneous stones exhibit visually distinct layers or regions characterized by different colors or textures. The LIBS spectra obtained from these visually disparate areas revealed the corresponding differences in the elemental profiles. This observation strongly suggests that formation process of these urinary stones was not uniform and likely inVol.ved sequential deposition or incorporation of materials with different chemical compositions at different stages of growth. This can lead to a complex internal structure, in which different regions of the same stone possess distinct elemental signatures.

The LIBS spectra obtained from multiple points on these samples clearly demonstrate intrastone variability, with certain elements showing strong emission lines in one location and being absent or significantly weaker in the other. This finding underscores the inherent limitations of characterizing the overall composition of macroscopically heterogeneous urinary stones based solely on a single-point analysis. Identifying the distinct elemental compositions in different regions of the same urinary stone has significant implications for understanding the complex pathogenesis of urolithiasis. This suggests that factors such as fluctuations in urine chemistry over time, presence of multiple nucleation sites with differing affinities for specific ions, and sequential precipitation of various mineral phases can contribute to the formation of intricate and chemically heterogeneous urinary calculi. Understanding heterogeneity may be crucial developing targeted and effective strategies to treat and prevent recurrent stone formation.

It is essential to emphasize that the LIBS analysis conducted in this study, as described in the provided source, primarily focused on the qualitative identification of the elemental constituents of the urinary stone samples. Although the strength of the spectral lines produced in LIBS is inherently linked to the

concentration of the respective element in the plasma, and consequently in the Vol.ume of the sample that has been ablated, conducting a precise quantitative elemental analysis requires sophisticated experimental more analytical methodology. This approach typically requires a series of well-characterized matrix-matched standard reference materials with known elemental compositions. analyzing these standards under experimental conditions identical to those of the unknown samples, calibration curves can be generated, allowing for the determination of elemental concentrations in the unknown samples. Therefore, the results presented herein should interpreted primarily providing as information on the elements present in the urinary stone samples, rather than their precise concentrations or relative abundances beyond what can be inferred from the number and intensity of the observed spectra. Future studies aiming for more precise quantification of the elemental composition of urinary stones using LIBS will require the development and application of appropriate calibration methodologies.

C. XRD Analysis of Urinary Stone Samples

complement the elemental performed using LIBS, XRD was employed to investigate the crystalline structure and mineralogical composition of a subset of the urinary stone samples. A total of 19 of the 40 samples analyzed by LIBS were subjected to XRD analysis. Prior to XRD analysis, the selected urinary stone samples were prepared. Following the initial LIBS analysis, the samples were ground into fine powder using an agate mortar and pestle to ensure homogeneity and diffraction conditions. Powdered samples were placed in sterile containers and subjected to XRD analysis. This powder form is required for XRD analysis to allow random orientation of crystallites, which is necessary for generating a representative diffraction pattern.

XRD analysis was performed using an X-ray diffractometer with an X-ray source, a sample holder, and a detector. The powdered sample was irradiated with an X-ray beam and the

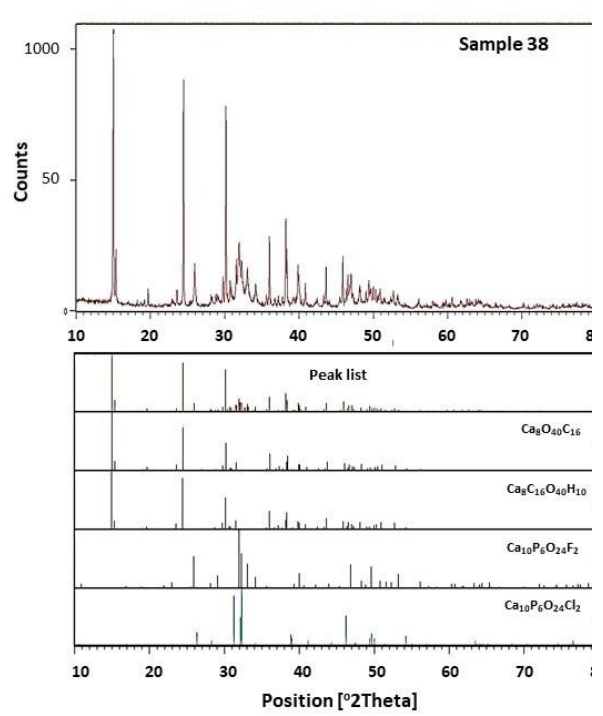


Fig. 5 XRD results identifying the crystalline components of Sample 38, mainly Whewellite and Fluorapatite

intensity of the diffracted X-rays was measured as a function of the diffraction angle (2 θ). The principle of XRD is based on the diffraction of X-rays by regularly spaced crystal lattice planes within a sample. Each crystalline phase exhibited unique diffraction a characterized by the positions (2θ values) and intensities of the diffraction peaks. Figure 5 presents the XRD analysis of sample 38, revealing that it is primarily composed of whewellite with a secondary presence of fluorapatite and potentially trace amounts of chlorapatite. This interpretation is based on the matching of peak positions between the sample diffraction pattern and the reference patterns provided. Table 1 lists the XRD and LIBS results for the selected samples. The XRD analysis identified various crystalline phases, including calcium, iron, magnesium, and organic compounds.

The XRD patterns of the urinary stone samples were analyzed by comparing them with standard diffraction patterns from reference databases. This comparison allowed the identification of the crystalline phases present in each sample. For instance, the XRD pattern

of sample number 1 revealed the presence of two crystalline units, identified as Calcium Oxalate Monohydrate (whewellite) with the chemical formula C2CaO4·H2O and Calcium Oxalate Dihydrate (raphide) with the chemical formula CaC₂O₄·2H₂O. Similarly, Sample 2 contained a single crystalline unit, cystine (C₆H₁₂N₂O₄S₂). Interestingly, several samples exhibited multiple crystalline phases, indicating heterogeneous mineralogical compositions. Sample 3, for example, comprised four distinct crystalline units: Calcium Oxalate Dihydrate (raphide), Calcium Carbonate (Calcite, CaCO₃), Iron Carbonate (Siderite, FeCO₃), and unidentified organic compound (C₁₀H₁₀N₆O₄). In contrast, sample 13 contained only one identifiable crystalline unit, Calcium Oxalate Dihydrate (raphide).

Furthermore, for Sample 23, which exhibited a distinct core and shell, separate XRD analyses were conducted on these two parts. The XRD results indicate that the core of sample 23 consisted solely of Calcium Oxalate Dihydrate (raphide). Conversely, the shell of sample 23 was identified as uricite (C₅H₄N₄O₃), an organic compound. This finding suggests compositional difference between the inner and outer layers of urinary stones. The results obtained from the XRD analysis provide crucial information regarding the mineralogical composition of the urinary stone samples. Identifying the specific crystalline phases present is essential for understanding the origin of stone formation, and can aid in determining appropriate treatment and prevention strategies for urolithiasis. The diverse range of crystalline components identified, including oxalates, carbonates, and organic compounds, such as uricite and cystine, highlights the complexity of urinary stone formation. The complementary use of XRD and LIBS allows for more comprehensive characterization of urinary stones, providing both elemental and structural information.

D. Significance of LIBS Findings for Understanding Urinary Stone Composition

The application of LIBS in this study has proven to be a valuable approach for gaining

detailed insight into the elemental composition of a diverse collection of urinary tract stones.

Table 1 XRD and LIBS results for selected samples, showing identified crystalline phases and elemental composition

Sample	T TDG D	WDD D L	
Number	LIBS Results	XRD Results	
3	N, Ca, Fe, Cr, Al, Na, O, Cu, Ar, C, H, Si, Ti.	C ₁₀ H ₆ CaN ₈ O ₆ (Calcium urate) Ca ₆ C ₆ O ₁₈ (Calcite), Fe ₆ C ₆ O ₁₈ (Siderite), Ca ₈ O ₄₀ C ₁₆ .	
11	Ca, N, Fe, Na, O, Si, Ti, Al, C, Cu, H.	Ca ₈ O ₄₀ C ₁₆ (Raphide), Ca(CO ₂) ₂ (H ₂ O) ₂₂ (Weddellite), CaC ₂ O ₄ H ₂ O (Whewellite), N ₄ C ₈ H ₁₂ .	
18	Ca, N, Mg, O, Na, Fe, K, H, P, Sr, Al, Cr, Cu.	Mg4S4O44H56 (Epsomite), CaCO3 (Vaterite), N ₁₆ H ₃₂ C ₂₄ , N ₄ H ₆₄ C ₁₄ O ₁₆ C ₂₈ , Na ₂ S ₂ O ₄ .	
26	Ca, N, Na, O, C, C, Fe, H.	Ca ₈ O ₄₀ C ₁₆ (Raphide), Ca ₄ O ₄ (Lime), C ₁₀ H ₈ N ₂ O ₂ .	
28	N, Fe, O, Ca, Na, Cu, H, C, Si, Ti, Cr.	C ₂₀ H ₁₆ N ₁₆ O ₁₂ (Uricite), Ca ₈ O ₄₀ C ₁₆ , C ₂ FeO ₄ H ₂ O, C ₄ H ₁₂ CuN ₂ O ₂ .	
30	Ca, N, O, C, Cu, Ti, Na, Si, Fe, H, Th, Mg, Al, Ar, Ba, Cr, Si, Sr.	CaC ₂ O ₄ H ₂ O (Whewellite).	
32	N, Ca, O, Cu, Fe, H, C, Na, Si, Sr, Ti, Cr, Mg, Sn, Al.	C ₂₀ H ₁₆ N ₁₆ O ₁₂ (Uricite), Ca6C ₆ O ₁₈ (Calcite).	
33	N, Ca, Fe, Ti, O, Si, K, Na, H, Mn, Ni, Zn, Cl, Cr, Cu, Ba, C, Al, P.	Na ₈ Al ₆ Si ₆ O ₂₄ (Sodalite), Si ₈ O ₁₆ (Cristobalite).	
35	Ca, N, Na, O, Si, C, Fe, H, Ti, Ar, Cr, Cu, Mo, Zn, Zr.	CaC ₂ O ₄ H ₂ O (Whe wellite), Ca ₆ C ₆ O ₁₈ , Calcite, Fe ₄ O ₂₈ C ₃₂ , Mg ₂ (PO ₄)F (Magniotriplite), N ₁₆ H ₃₂ C ₂₄ .	
36	Ca, N, Fe, O, Na, H, C, Si, Cu, K, Ti, Al, Ar, Br.	Ca ₈ O ₄₀ C ₁₆ (Raphide), C ₂₀ H ₁₆ N ₁₆ O ₁₂ (Uricite).	
37	N, Fe, O, Na, Cu, Ca, C, Cr, Ti, H, Mg, Pd, Si, Ar, Mg, Mn, P.	C ₂₀ H ₁₆ N ₁₆ O ₁₂ (Uricite), Ca ₆ C ₆ O ₁₈ (Calcite).	
39	N, Fe, Ca, Na, C, O, H, Ar, P, Si, Ti, Zn, Cr, Cu, Pd, K, Mg, Al.	$C_{20}H_{16}N_{16}O_{12}$ (Uricite).	

The analysis of macroscopically uniform stones revealed a consistent suite of constituent elements, with sodium, calcium, and nitrogen

as consistently prominent components. This information contributes to our understanding of fundamental building blocks the homogeneous calculi. Furthermore, the investigation of macroscopically heterogeneous stones yielded a significant finding of substantial intra-stone variability observation elemental composition. This highlights the complex and dynamic nature of the processes inVol.ved in urinary stone The development. presence of distinct elemental signatures in different regions of the same stone suggests that these stones may have formed through sequential deposition of different mineral phases or under fluctuating biochemical conditions within the urinary tract. The detection of additional elements, such as Mn, Mo, Ni, and Br, in some heterogeneous samples and their localized distribution further underscores this complexity.

The findings from the LIBS analysis, particularly the identification of elemental heterogeneity within individual stones. complement the results obtained from structural analysis techniques, such as XRD, which was employed in this study. While XRD provides information about the crystalline phases present in the stones, LIBS offers a direct measure of the elemental composition, including both elements incorporated within the crystalline structures and those that might be present in amorphous or trace amounts.

Utilizing these complementary analytical methods together offers a more thorough characterization of urinary stone composition. This comprehensive approach can enhance the understanding of the root causes of urolithiasis and guide the development of more effective strategies for its diagnosis, treatment, and prevention. The ability of LIBS to rapidly provide elemental information with minimal sample preparation, particularly regarding heterogeneity within stones, makes it a powerful tool for the study of urinary calculi.

IV. CONCLUSION AND REMARKS

This study provides a detailed analysis of urinary tract stones from 40 patients in Yazd Province, Iran, using LIBS for elemental identification and XRD for crystalline structure integration of determination. The techniques allowed for a comprehensive characterization of stone composition. This study identified key crystalline components, such as calcium oxalate dihydrate (in the forms of Whewellite, Wheddellite, and Raphide) and calcium carbonate (Calcite and Vaterite), as well as the presence of uric acid (uricite)¹. A significant finding was the heterogeneity observed within certain stone samples, indicated by varying elemental compositions across different points on the stone surface via LIBS and differing crystalline structures between the core and shell of some stones, as analyzed using XRD. The novelty of this study lies in its specific focus on patients from Yazd Province, providing region-specific insights into the types of urinary stones prevalent in this area. The methodological rigor of this study, including the separate XRD analysis of the core and shell regions and the application of multipoint LIBS, offers a more in-depth understanding of stone formation than simple bulk analysis.

Future research should focus on larger-scale studies within Yazd and comparative analyses with other regions to establish a more statistically significant understanding of the stone-type distribution. Correlating stone composition with comprehensive patientspecific data (age, sex, medical history, diet, and lifestyle) is crucial for identifying the relevant risk factors in the Yazd population. Future studies should also aim to implement quantitative analytical methods for both LIBS XRD to obtain precise elemental concentrations and phase percentages of the Further investigation minerals. of heterogeneous nature of stones using advanced imaging techniques, such as micro-CT coupled with spatially resolved LIBS and XRD, can

¹ The term "raphide" specifically refers to the needle-like crystal habit of calcium oxalate dihydrate, while "Wheddellite" is the mineral name for the same chemical compound.

provide insights into stone formation mechanisms. Additionally, analyzing the composition of local water sources and comparing them with stone elemental profiles could reveal potential environmental contributions.

The findings are significant for patients in Yazd Province, providing initial evidence of common urinary stone types in this region, which can inform clinical diagnostic and treatment considerations in hospitals, such as Shahid Rahnamoun. The identified prevalence of calcium oxalate, calcium carbonate, and uric acid stones suggests that standard management strategies for these stones are likely applicable. The observation of heterogeneity within stones has important implications for treatment because stones with different core and shell compositions may require tailored approaches for effective management. Future research correlating stone composition with treatment outcomes can help refine clinical guidelines in Yazd. Detailed elemental analysis by LIBS could uncover region-specific trace elements and their potential link to metabolic disorders or environmental risk factors, paving the way for targeted preventive measures and improving patient management strategies specific to the Yazd Province. This study represents an important initial step towards a better understanding of urolithiasis.

ACKNOWLEDGMENT

The authors express their sincere gratitude to Yazd Shahid Rahnemuon Hospital and its surgical department for their generous collaboration in providing the kidney stone samples essential for this study.

V. REFERENCES

- [1] S. Jaswal and V. K. Singh, "Analytical assessments of gallstones and urinary stones: a comprehensive review of the development from laser to LIBS," Appl. Spectrosc. Rev., Vol. 50, no. 6, pp. 473-498, 2015.
- [2] V. Unnikrishnan, R. Nayak, S. Bhat, S. Mathew, V. Kartha, and C. Santhosh, "Biomedical applications of laser-induced breakdown spectroscopy (LIBS)," in Optical Diagnostics and Sensing XV: Towards Point-

- of-Care Diagnostics, 2015, Vol. 9332: SPIE, pp. 158-162.
- [3] F.S. Muhammed, M.I. Salih, R.A. Omer, A.F. Qader, R.F. RashidIman, and E.I. Abdulkareem, "A review: evaluating methods for analyzing kidney stones and investigating the influence of major and trace elements on their formation," Rev. Inorg. Chem., Vol. 45, pp. 307-319, 2025.
- [4] C. Grant, G. Guzman, R.P. Stainback, R.L. Amdur, and P. Mufarrij, "Variation in Kidney Stone Composition Within the United States," J. Endourol., Vol. 32, no. 10, pp. 973-977, 2018.
- [5] A. Kubala-Kukuś, M. Szczerbowska-Boruchowska, A. Dudek, A. Woźniak, and J. Lekki, "Application of TXRF and XRPD techniques for analysis of elemental and chemical composition of human kidney stones," X-Ray Spectrom., Vol. 46, no. 5, pp. 412-420, 2017.
- [6] V. Castiglione, P.-Y. Sacre, E. Cavalier, P. Hubert, R. Gadisseur, and E. Ziemons, "Raman chemical imaging, a new tool in kidney stone structure analysis: Case-study and comparison to Fourier Transform Infrared spectroscopy," PloS one, Vol. 13, no. 8, pp. 0201460(1-18), 2018.
- [7] S. J. Rehse, *Biomedical applications of LIBS*, in Laser-Induced Breakdown Spectroscopy: Theory and Applications: Springer, pp. 457-488, 2014.
- [8] N.G. Hokamp, S.R. Leng, A.F. Halaweish, R.L. Ehman, and C.H. McCollough, "Low-dose characterization of kidney stones using spectral detector computed tomography: an ex vivo study," Investig. Radiol., Vol. 53, no. 8, pp. 457-462, 2018.
- [9] A. Ferrero, R. Gutjahr, A.F. Halaweish, S. Leng, and C.H. McCollough, "Characterization of urinary stone composition by use of whole-body, photon-counting detector CT," Acad. Radiol., Vol. 25, no. 10, pp. 1270-1276, 2018.
- [10] S. Sarmani, L. Kuan, and M. Bakar, "Instrumental neutron activation analysis of kidney stones," Biolog. Trace Element Res. Vol. 26, pp. 497-502, 1990.
- [11] A. Aleksandrova, A.V. Pakhomov, A.V. Derbenev, A. A. Burmistrov, and A.V. Shishkov, "Elemental composition of single-phase kidney stones. Part II," in J. Phys.: Conf.

- Ser., 2021, Vol. 1989, no. 1: IOP Publishing, p. 012013.
- [12] C. Pineda, A. Rodgers, V. Prozesky, and W. Przybylowicz, "Elemental mapping analysis of recurrent calcium oxalate human kidney stones," Nucl. Instrum. Methods Phys. Res. Sect. B: Beam Interact. Mater. Atoms, Vol. 104, no. 1-4, pp. 351-355, 1995.
- [13] R. Izan, M.A. Haddad, and M. Borhani Zarandi, "Elemental Analysis of Asphaltene Sediments Extracted from Oil Wells at the Southwest of Iran by Laser-Induced Breakdown Spectroscopy," J. Pet. Res., Vol. 34, no. 1403-1, pp. 140-149, 2024.
- [14] N. Sedighi and M. Haddad, "Elemental analysis of air-full dust in world heritage city of Yazd by laser induced breakdown spectroscopy," J. Earth Space Phys., Vol. 47, no. 1, pp. 127-144, 2021.
- [15] N. Mutlu, S. Çiftçi, T. Gülecen, B.G. Öztoprak, and A. Demir, "Laser-induced breakdown spectroscopy is a reliable method for urinary stone analysis," Turk. J. Urol., Vol. 42, no. 1, pp. 21-27, 2016.
- [16] S. Rehse, H. Salimnia, and A. Miziolek, "Laser-induced breakdown spectroscopy (LIBS): an overview of recent progress and future potential for biomedical applications," J. Med. Eng. Technol., Vol. 36, no. 2, pp. 77-89, 2012.
- [17] R. Gaudiuso and N. Melikechi, "Minimally invasive medical diagnosis through Laser-Induced Breakdown Spectroscopy (LIBS) coupled with machine learning," in 2022 Photonics North (PN), 2022: IEEE, pp. 1-1.
- [18] K. Muhammed Shameem, S. Sreedhar, P.S. Sreedevi, N.V. Unnikrishnan, and C.P.G. Vallabhan, "Laser-induced breakdown spectroscopy-Raman: An effective complementary approach to analyze renalcalculi," J. Biophotonics, Vol. 11, no. 6, pp. 201700271(1-13), 2018.
- [19] B. G. Oztoprak, N. Mutlu, S. Çiftçi, T. Gülecen, and A. Demir, "Analysis and classification of heterogeneous kidney stones using laser-induced breakdown spectroscopy (LIBS)," Appl. Spectrosc., Vol. 66, no. 11, pp. 1353-1361, 2012.
- [20] A.A. I. Khalil, M.A. Gondal, M. Shemis, and I.S. Khan, "Detection of carcinogenic metals in kidney stones using ultraviolet laser-induced

- breakdown spectroscopy," Appl. Opt., Vol. 54, no. 8, pp. 2123-2131, 2015.
- [21] V.K. Singh, A. Rai, P. Rai, and P. Jindal, "Cross-sectional study of kidney stones by laser-induced breakdown spectroscopy," Lasers Med. Sci., Vol. 24, pp. 749-759, 2009.
- [22] A.K. Pathak, R. Kumar, V.K. Singh, R. Agrawal, S. Rai, and A.K. Rai, "Assessment of LIBS for spectrochemical analysis: a review," Appl. Spectrosc. Rev., Vol. 47, no. 1, pp. 14-40, 2012.
- [23] P. Khalili, A. Hashemi, M. Fallahzadeh, M. Koochakzadeh, and A. Afshinfar, "Risk factors of kidney stone disease: a cross-sectional study in the southeast of Iran," BMC Urol., Vol. 21, pp. 1-8, 2021.
- [24] S. Shahidi, S. Dolatkhah, M. Mortazavi, A. Atapour, F. Aghaaliakbari, R. Meamar, M. Badri, and D. Taheri "An epidemiological survey on kidney stones and related risk factors in the Iranian community," Acta Med. Iranica, Vol. 60, pp. 307-312, 2022.
- [25] T. Zahirian Moghadam, F. Pourfarzi, H. Mohseni Rad, and H. Zandian, "Kidney stones among Iranian adults: Prevalence and socioeconomic inequality assessment in a cohort-based cross-sectional study," Health Sci. Rep., Vol. 5, no. 6, pp. 877(1-9), 2022.
- [26] F. Khaleghi, R. Rasekhi, and M. Mosaferi, "Mineralogy and elemental composition of urinary stones: A preliminary study in northwest of Iran," Period. Mineral., Vol. 90, no. 1, pp. 105-119, 2021.
- [27] B. Keshavarzi, N. Yavarashayeri, D. Irani, F. Moore, A. Zarasvandi, and M. Salari, "Trace elements in urinary stones: a preliminary investigation in Fars's province, Iran," Environ. Geochem. Health, Vol. 37, pp. 377-389, 2015.
- [28] J. Moludi, H. Lateef Fateh, Y. Pasdar, M. Moradinazar, L. Sheikhi, A. Saber, N. Kamari. M. Bonyani, F. Najafi, and P. Dey "Association of dietary inflammatory index with chronic kidney disease and kidney stones in Iranian adults: a cross-sectional study within the Ravansar non-communicable diseases cohort," Front. Nutr., Vol. 9, pp.. 955562(1-8), 2022.
- [29] A. Kramida, Y. Ralchenko, and J. Reader, "NIST ASD team nist atomic spectra database (ver. 5.7. 1)," National Institute of Standards and Technology, Gaithersburg, MD, 2015.



Rezvan Babamir earned a BSc in Atomic Physics from Yasuj University in 2019 and subsequently obtained an MSc in Optics and Laser Physics from Yazd University. During her research tenure at the Laser Spectroscopy Research Laboratory (LSRL) from 2021 to 2024, her work focused on the application of laser technologies to advance medical sciences.



Mohammad Ali Haddad is an Assistant Professor of Atomic and Molecular Physics at Yazd University, with expertise in Optics, Lasers, and Spectroscopy. His research program encompasses applied nonlinear optics, molecular physics, and laser applications. Dr. Haddad's doctoral research at VU Amsterdam and Leiden University focused on high-resolution laser spectroscopy, contributing to the understanding of diffuse interstellar bands. He also holds an MSc in Atomic and Molecular Physics from Yazd University, where his work involved experimental studies of multiphoton absorption and dissociation.



Seyed Hassan Tavassoli is a Professor at the Laser and Plasma Research Institute, Shahid Beheshti University, Tehran, Iran. He holds a PhD and a Master's degree in Physics from

Shahid Beheshti University (awarded in 2003 and 1997, respectively) and a Bachelor's degree in Physics from Isfahan University of Technology (1994). His research interests lie within the field of laser and plasma. He has previously served as the Head and Vice-Dean for Research at the Laser and Plasma Research Institute, as well as the Head of the Laser Applications Group.



Mohamad Reza Samadzadeh Yazdi holds a PhD in Mineral Processing from Tarbiat Modares University (2013), preceded by a Master's degree in the same field from the same university (2008) and a Bachelor's degree in Mining Engineering from Yazd University (2005). He currently manages the Mineral Processing Group at the Mining Technologies Research Center (MTRC), Yazd University, Iran.



Serajuddin Vahidi is a specialist urologist with a medical degree from Isfahan University of Medical Sciences (1984) and a specialty doctorate from Shahid Beheshti University of Medical Sciences (1993). He has practiced surgery at Shahid Rahnemoun Hospital since 1994 and has held leadership roles as Head of Urology at Shahid Sadoughi University, Yazd, Itan and Head of the Endourology Research Center.

THIS PAGE IS INTENTIONALLY LEFT BLANK.